Climate
of the Past

Open Access

Climate variability over the last 92 ka in SW Balkans from analysis of sediments from Lake Prespa

K. Panagiotopoulos[1]**, A. Böhm**[2]**, M. J. Leng**[3,4]**, B. Wagner**[2]**, and F. Schäbitz**[1]

[1]Seminar of Geography and Education, University of Cologne, Gronewaldstraße 2, 50931 Cologne, Germany
[2]Institute of Geology and Mineralogy, University of Cologne, Zülpicher Straße 49a, 50674 Cologne, Germany
[3]Centre for Environmental Geochemistry, School of Geography, University of Nottingham, Nottingham, NG7 2RD, UK
[4]NERC Isotope Geosciences Laboratory, British Geological Survey, Nottingham, NG12 5GG, UK

Correspondence to: K. Panagiotopoulos (panagiotopoulos.k@uni-koeln.de)

Abstract. The transboundary Lake Prespa (Albania/former Yugoslav Republic of Macedonia/Greece) has been recognized as a conservation priority wetland. The high biodiversity encountered in the catchment at present points to the refugial character of this mountainous region in the southwestern Balkans. A lake sediment core retrieved from a coring location in the northern part of the lake was investigated through sedimentological, geochemical, and palynological analyses. Based on tephrochronology, radiocarbon and electron spin resonance (ESR) dating, and cross correlation with other Northern Hemisphere records, the age model suggests that the basal part of core Co1215 reaches back to 92 ka cal BP. Here we present the responses of this mid-altitude site (849 m a.s.l.) to climate oscillations during this interval and assess its sensitivity to millennial-scale variability. Endogenic calcite precipitation occurred in marine isotope stages (MIS) 5 and 1 and is synchronous with periods of increased primary production (terrestrial and/or lacustrine). Periods of pronounced phytoplankton blooms (inferred from green algae and dinoflagellate concentrations) are recorded in MIS 5 and MIS 1 and suggest that the trophic state and lake levels underwent substantial fluctuations. Three major phases of vegetation development are distinguished: the forested phases of MIS 5 and MIS 1 dominated by deciduous trees with higher temperatures and moisture availability, the open landscapes of MIS 3 with significant presence of temperate trees, and the pine-dominated open landscapes of MIS 4 and MIS 2 with lower temperatures and moisture availability. Our findings suggest significant changes in forest cover and landscape openness, as well as in the properties of the vegetation belts (composition and distribution) over the period examined. The study area most likely formed the upper limit of several drought-sensitive trees (temperate tree refugium) at these latitudes in the Mediterranean mountains.

1 Introduction

The Balkan Peninsula has very heterogeneous habitats, landscapes, and climate (Grove and Rackham, 2003). This heterogeneity has shaped the fauna and flora through time and accounts for the impressive floral and faunal biodiversity also found on the Iberian and Italian peninsulas (Blondel et al., 2010). These three Mediterranean peninsulas, in particular the Balkans, are thought to have provided shelter for species over recurring glacial–interglacial cycles (Griffiths et al., 2004).

A recent review of the vegetational response in Europe during the last glacial (Fletcher et al., 2010) demonstrated that millennial-scale events, such as Dansgaard–Oeschger (D–O) cycles and Heinrich (H) events, are clearly identifiable in both terrestrial and marine pollen diagrams. Two features are apparent from this regional review of MIS 4 to MIS 2. Firstly, long and continuous sequences registering millennial-scale variability during this period are located almost exclusively within the Mediterranean region. Indeed, owing to its latitudinal location, this region has provided exceptional records that span several glacial cycles such as the renowned pollen sequence of Tenaghi Philippon (Wijmstra, 1969). The second feature is the relative high density of long
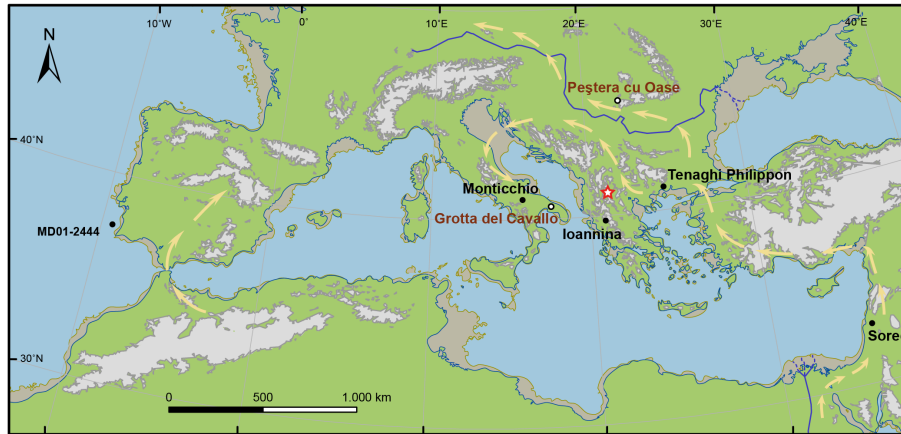
Fig. 1. Locations of the records described, including Lake Prespa (star); archaeological sites are marked with an open circle. Note the paleo-coastline during MIS 3 at 100 m below present sea level (in beige) and possible dispersal routes of modern humans (arrows).

pollen records in the southern Balkans. Several continuous pollen sequences encompassing multiple glacial cycles have been obtained from Greece (Wijmstra, 1969; Okuda et al., 2001; Tzedakis et al., 2002). Some of them confirm the notion of glacial refugia for temperate trees (e.g., the Ioannina basin located in northwestern Greece). There are no pollen records covering the last glacial cycle outside Greece, with the exception of Lake Ohrid (on Albania–FYR of Macedonia border) (Lézine et al., 2010). However, most cores retrieved from the latter reveal disruptions in the sedimentation patterns (Vogel et al., 2010; Lézine et al., 2010).

The relative abundance of paleo-vegetation archives spanning the last glacial existing in the vicinity of Lake Prespa allows the examination of intra-regional patterns of environmental and climatic conditions. The late-glacial pollen record from Lake Prespa (Fig. 1) provides insights into the vegetation and climate conditions at a centennial-scale from an altitude of 849 m a.s.l. (Aufgebauer et al., 2012; Panagiotopoulos et al., 2013). Ensuing isotopic and hydrological studies on a ∼ 16 m core (Co1215) confirmed the sensitivity of the site to climate variability (Wagner et al., 2012; Leng et al., 2013), and a recent lithological and tephrostratigraphical study on a ∼18 m long core (after the addition of 2 m to the composite core Co1215 retrieved in 2011) indicates that the sediment accumulation in the central northern part of the lake is undisturbed and covers the last c. 92 ka cal BP (Damaschke et al., 2013).

Here we present sedimentological, geochemical and palynological data of core Co1215 with a focus on biological proxies and ecological processes. Our multi-proxy approach aims at understanding the complex responses of the Lake Prespa catchment to climate variability during the last glacial. In order to assess the impacts of orbital- and suborbital-scale variability we first examine the response of the study area on a local level, and then compare it to selected regional and global reference archives. Finally, we discuss

implications of the climate reconstruction for modern human dispersal into Europe and other environmental constraints posed on hominid migrations/populations.

2 Physical setting

The Prespa Lakes (Megali and Mikri Prespa) and the surrounding streams and springs, enveloped by mountains forming several peaks around or above 2000 m a.s.l., are shared between Albania, the former Yugoslav Republic of Macedonia, and Greece (Fig. 2). Lake Megali Prespa, hereafter referred to as Lake Prespa, has no surface outflow and is separated by an alluvial isthmus from Lake Mikri Prespa. The lake has a catchment area of 1300 km^2, a mean water depth of 14 m (48 m maximum), and a surface area of 254 km^2 (Matzinger et al., 2006). Lake Prespa is situated at 849 m a.s.l. and drains through karst channels traversing the Galičica and Mali Tate mountains into Lake Ohrid standing at 693 m a.s.l. Hence, it belongs hydrologically to the Adriatic drainage region, although recent faunal studies suggested a closer biogeographical affiliation with lakes eastwards belonging to the Aegean drainage region (Wilke et al., 2010).

The geology of the area mainly comprises granites and Mesozoic limestones. The climate is transitional and can be classified as sub-Mediterranean with continental influences. Mean July and January temperatures in the lowlands are 21 and 1 °C, respectively, with a mean annual temperature of 11 °C. Precipitation varies from 750 mm in the lowlands to over 1200 mm in the mountains, and peaks in winter when snowfalls are frequent (Hollis and Stevenson, 1997). Consequently, streams and springs are fed by late spring snowmelt, resulting in peak lake levels in May and June. Total inflow comprises stream and spring discharge (56 %), direct precipitation (35 %) and Mikri Prespa inflow (9 %). In the absence of natural surface outlet, water from Lake Prespa is mostly evaporated (52 %), fed through the karst aquifer (46 %) to

Fig. 2. Topography of Lake Prespa. Lake catchment (blue line) and core locations (Co1215, this study) are shown (SRTM Data: Jarvis et al., 2008).

the water column, leading, in concert with geostrophic effects, to the formation of a contourite drift (Wagner et al., 2012).

The diverse topography of the Lake Prespa catchment and its location at a transitional climate zone gave rise to an assemblage of central European, Mediterranean and Balkan endemic plant species (Polunin, 1980). The major vegetational formations encountered at Prespa, in descending order, are the alpine and subalpine meadows, the montane conifer forests (notably *Pinus peuce* forests), the montane deciduous forests (dominated by *Fagus sylvatica*), the mixed deciduous oak forests (with thermophilous species closer to the lake) and the grasslands of the littoral zone. Panagiotopoulos et al. (2013) described the diversity and origin of the modern flora found at Prespa and discussed the refugial character of the study site.

3 Material and methods

Here we present a data set of core Co1215 (40°57′50″ N, 20°58′41″ E) with a composite length of 1776 cm recovered from a location at the northern part of Lake Prespa (14.5 m water depth) in November 2009 and June 2011 (Fig. 2). The coring location displays relatively undisturbed sedimentation, revealed after a shallow hydroacoustic survey (Wagner et al., 2012). The core was recovered from a floating platform equipped with a gravity corer for surface sediments and a 3 m long percussion piston corer for deeper sediments (UWITEC Co. Austria). One core half was used for non-destructive analyses (e.g., XRF scanning) and then archived at the Institute of Geology and Mineralogy at the University of Cologne, Germany; the other half was subsampled at 2 cm intervals and the samples were freeze-dried and homogenized using an agate ball mill. The core comprises mostly grayish bioturbated silts with sporadic occurrences of coarser sands and gravels.

3.1 Geochemical analyses

X-ray fluorescence (XRF) scanning was performed at 2 mm steps with an analysis time of 10 s per measurement using an ITRAX core scanner (COX Analytical Systems, Sweden). The count rates of individual elements presented here were used as semi-quantitative estimates of their relative concentrations (for more details see Aufgebauer et al., 2012). Total carbon (TC) and total inorganic carbon (TIC) were measured with a DIMATOC 200 (DIMATEC Ltd. UK) and total organic carbon (TOC) was calculated by subtracting TIC from TC. Concentrations of total nitrogen (TN) were measured with a Vario Micro Cube combustion CNS elemental analyzer (VARIO Co.). The atomic TOC/TN ratio (abbreviated as C/N) was quantified in order to identify the source of the organic matter in the lake sediments (cf. Meyers and Ishiwatari, 1995). The identification of carbonate types (e.g.,

Ohrid springs, and 2 % is used for irrigation (Matzinger et al., 2006). Increasing anthropogenic pressure combined with precipitation patterns and the closed nature of the watershed account for the interannual lake level change and an estimated residence time of 11 years (Matzinger et al., 2006). Apart from seasonal variations, lake levels have oscillated historically (up to several meters) as evidenced by existing national records and inundated settlement ruins from the 11th century (Wagner et al., 2012). Level fluctuations of Lake Prespa are expected to influence the sedimentation regime given the shallow water depth with reference to the large surface area. At present, Lake Prespa is a mesotrophic lake and overturning of the water column has been documented to occur between the fall and spring, while thermal summer stratification results in dissolved oxygen depletion below 15 m (Matzinger et al., 2006). However, the lake underwent substantial changes in its trophic, mixing and level status in the past (Aufgebauer et al., 2012). The presence of gyres on the surface of Lake Prespa is assumed to propagate currents in

calcite, siderite) was determined by X-ray diffraction (XRD) analysis (Leng et al., 2013).

3.2 Palynological analyses

Palynological analyses were performed on 170 subsamples taken at 2–16 cm intervals. After measuring their volume, samples were sieved (112 μm), *Lycopodium* tablets (Stockmarr, 1971) were added in order to calculate concentrations, and subsequently they were processed using standard palynological techniques. Identification of palynomorphs was performed with relevant keys and atlases, as well as the reference collection of the Cologne Paleoecology (COPA) research group at the University of Cologne (Panagiotopoulos et al., 2013; and references therein). An average of 500 (with a minimum of 300) terrestrial pollen grains were counted per sample (with the exception of two samples at 546 and 890 cm, with a pollen sum of 171 and 177, respectively). The average temporal resolution between pollen samples, derived from the presented age model, is ∼500 years (ranging between 50 and 1250 years). Relative percentages were based on the sum of terrestrial pollen (excluding aquatics and spores). The term aquatics (or aquatic vegetation) in this study comprises vascular plants (macrophytes) and phytoplankton comprising green algae and dinoflagellates. The latter are presented in concentrations and the former both in concentrations and percentages based on a pollen sum including the main pollen sum and aquatics. Nomenclature and taxa group terminology follows Panagiotopoulos et al. (2013). Apart from *Artemisia*, which is plotted separately, the Asteraceae curve comprises differentiated Asteroideae, Cichorioideae and *Centaurea jacea*-type pollen percentages. Poaceae includes both Poaceae (wild types) and Cerealia (cultivars > 40 μm). Although *Phragmites* pollen grains were not differentiated, the modern vegetation of Prespa suggests that *Phragmites* grains must form part of the Poaceae (wild type) group. *Quercus* comprises differentiated deciduous (*Quercus robur*-type and *Quercus cerris*-type) and evergreen types.

The *Pediastrum* species encountered (*P. boryanum* spp., *P. simplex*) are freshwater planktic green algae, which have a cosmopolitan distribution and wide ecological tolerance (Komárek and Jankovská, 2001). Both species are dominant in eutrophic lakes under temperate climates, although the latter is also commonly found in tropical regions (Komárek and Jankovská, 2001). *Botryococcus* species are dominated by *B. braunii*, mostly in association with *B. neglectus* and *B. pila*. The synchronous occurrence of *Pediastrum* and *Botryococcus* species is characteristic of large eutrophic lakes with open water surface and extensive submerged and littoral vegetation typical for climatic optima (Jankovská and Komárek, 2000).

Dinoflagellate cysts were counted from the pollen slides and are attributed (tentatively) to *Gonyaulux*-type. Two morphotypes were distinguished: a dominant one with pronounced and protruding ornamentation present throughout the core and one with very limited or absent ornamentation and intermittent presence. Further studies (including SEM imaging) are needed to determine the species. Kouli et al. (2001) reported the presence of two identified freshwater dinoflagellates (*Gonyaulux apiculata* and *Spiniferites cruciformis*) from Lake Kastoria, northwestern Greece. As this lake is situated 20 km southwards from Lake Prespa, it is assumed the dinoflagellates encountered at Prespa (*Gonyaulux*-type) belong to *G. apiculata*.

3.3 Chronology

The age model of core Co1215 is based on accelerator mass spectrometry (AMS) ^{14}C dates, tephrochronology, electron spin resonance (ESR) dating and cross correlation with the NGRIP ice core record (NGRIP Members, 2004) and described in detail in Damaschke et al. (2013) (Fig. 3). Radiocarbon dates were calibrated (a cal BP) using the INTCAL09 calibration curve (Reimer et al., 2009) and for the uppermost sample using the Levin14c data set (Levin and Kromer, 2004). All ages presented in this paper are calendar ages. Aufgebauer et al. (2012), Wagner et al. (2012) and Damaschke et al. (2013) elaborate on the composition and correlation of the identified tephra layers, as well as on the ESR dating of a shell horizon at 1458–1463 cm. The ESR dating provided the only independent chronological tie-point below 858 cm (representing the last identified tephra layer) in core Co1215. Two additional tie-points below the ESR dated horizon, demarcating the maximum age of the lowermost part of the core, were fixed by tuning two TOC peaks to Dansgaard–Oeschger (D–O) warming events 21 and 22 of the NGRIP GICC05modelext (Damschke et al., 2013). According to the proposed age model, the base of the sediment sequence can be extrapolated to c. 92 ka cal BP.

4 Results

The upper 320 cm of core Co1215, spanning the past 17 ka, were described using lithology, geochemistry and chronology in Aufgebauer et al. (2012) and using palynological and microscopic charcoal data in Panagiotopoulos et al. (2013). Wagner et al. (2012) and Leng et al. (2013) presented sedimentological and geochemical data for the upper 1576 cm and provided some first age estimations of the sequence. This study presents sedimentological, palynological, and geochemical parameters for the longest (1776 cm) composite core to date, after the addition of 2 m recovered during fieldwork in June 2011.

Considering the distinct and overlapping lithological and palynological units, the ensuing discussion utilizes the marine isotope stages (MIS) chronological framework (Lisiecki and Raymo, 2005) to facilitate comparison between different proxies as well as other regional or global archives.
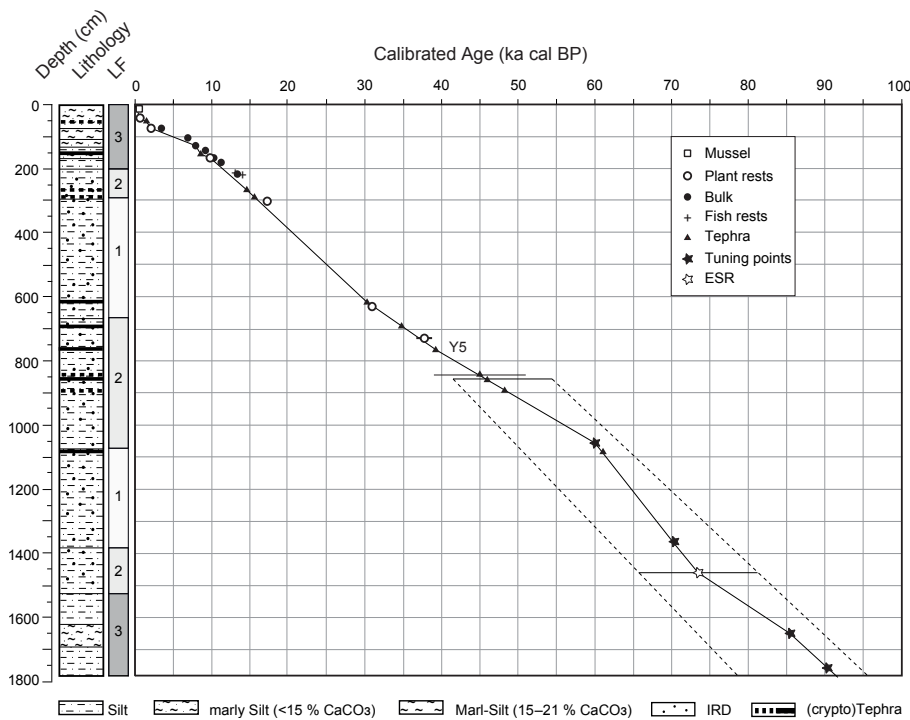
Fig. 3. Age model of core Co1215 with lithology. Reliable age control points were interpolated on a linear basis.

4.1 Lithology and geochemistry

Three lithofacies (L3, L2, L1) occur in Co1215, and have been distinguished based on color, grain-size composition and chemistry (Fig. 3). Lithofacies 3 (1776–1516 and 204–0 cm) sediments are characterized by olive-brown colored bioturbated silt, relatively high organic matter and calcium carbonate (calcite) and low to intermediate clastic content. Lithofacies 2 (L2; 1516–1380, 1066–662, and 292–204 cm) has grey-olive, non-laminated silts with intermediate organic content, and generally low carbonate content but with distinct TIC (calcite and siderite) and Fe spikes. Sporadic occurrence of sand and gravel was recorded in L2. Lithofacies 1 (L1; 662–292 and 1380–1066 cm) sediments are gray, bioturbated, dominated by silt and with very low organic content. Conspicuous TIC (siderite) and (Fe) spikes are present between 1380 and 1066 cm, and an irregular black-greenish lamination associated with black spots and high Fe and Mn (between 662 and 292 cm). Coarse sand and gravel were present intermittently throughout L1.

4.2 Pollen assemblage zones (PAZ)

Ten local pollen assemblage zones (P-1 to P-10) and several subzones were delimited based on visual inspection of the pollen record and supported by CONISS (constrained incremental sums of squares) cluster analysis for pollen taxa (> 2 %), included in the pollen sum as implemented by the TILIA pollen data spreadsheet program (Grimm, 1992).

Zone numbers and letters were assigned with ascending order from top to bottom (Fig. 4). The development of the palynoflora within the pollen assemblage zones and subzones identified at Prespa (Fig. 4) are summarized along with lithology, geochemistry and a brief description of the inferred paleo-environment at Prespa in Table 1. Subzones spanning the late glacial and the Holocene (P-2b to P-1a) are described in Panagiotopoulos et al. (2013).

5 Discussion

5.1 The Prespa paleo-archive

5.1.1 Vegetational and limnological responses to climate variability through space and time

The pollen record (Fig. 4) reveals two distinct phases (P-10 and P-8b) of high and sustained arboreal pollen percentages (mean AP > 75 %) at the base and one (P-1) at the top of core Co1215. During these intervals, deciduous trees dominated the pollen spectra and displaced *Pinus*. High percentages of *Abies*, *Quercus*, *Carpinus*, *Fagus*, and of other deciduous trees point to sufficient moisture availability and temperatures for growth. According to the age model, P-10 and P-8b correspond to MIS 5 (c. 92–71 ka cal BP) and P-1 to MIS 1 (Holocene). The forested landscape inferred is substantiated by high arboreal pollen concentration (proportional to tree population density) and low to intermediate
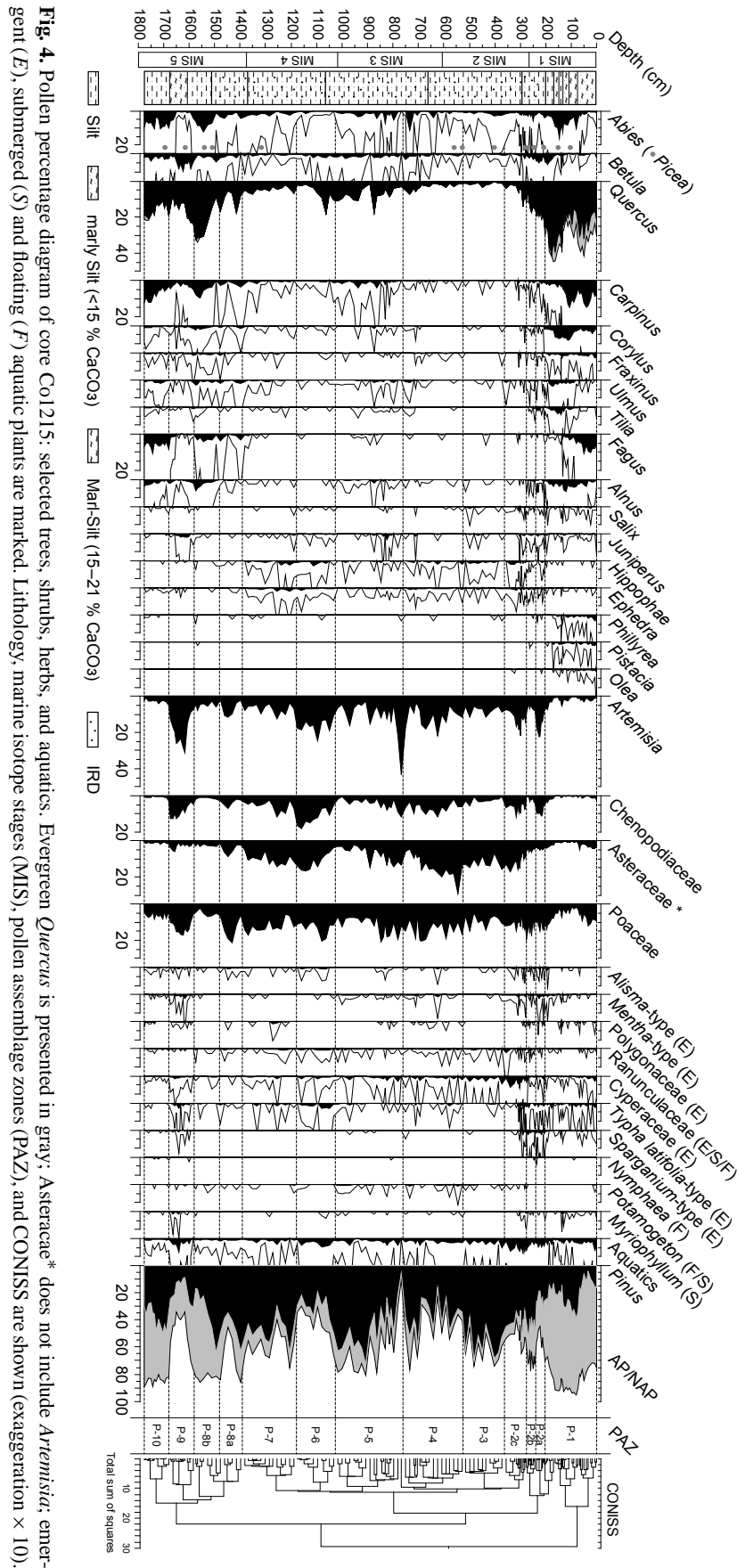
Fig. 4. Pollen percentage diagram of core Co1215: selected trees, shrubs, herbs, and aquatics. Evergreen *Quercus* is presented in gray; Asteracae* does not include *Artemisia*; emergent (*E*), submerged (*S*) and floating (*F*) aquatic plants are marked. Lithology, marine isotope stages (MIS), pollen assemblage zones (PAZ), and CONISS are shown (exaggeration × 10).

Table 1. Pollen assemblage zones (PAZ) in Co1215, including lithology, geochemistry and inferred paleo-environment.

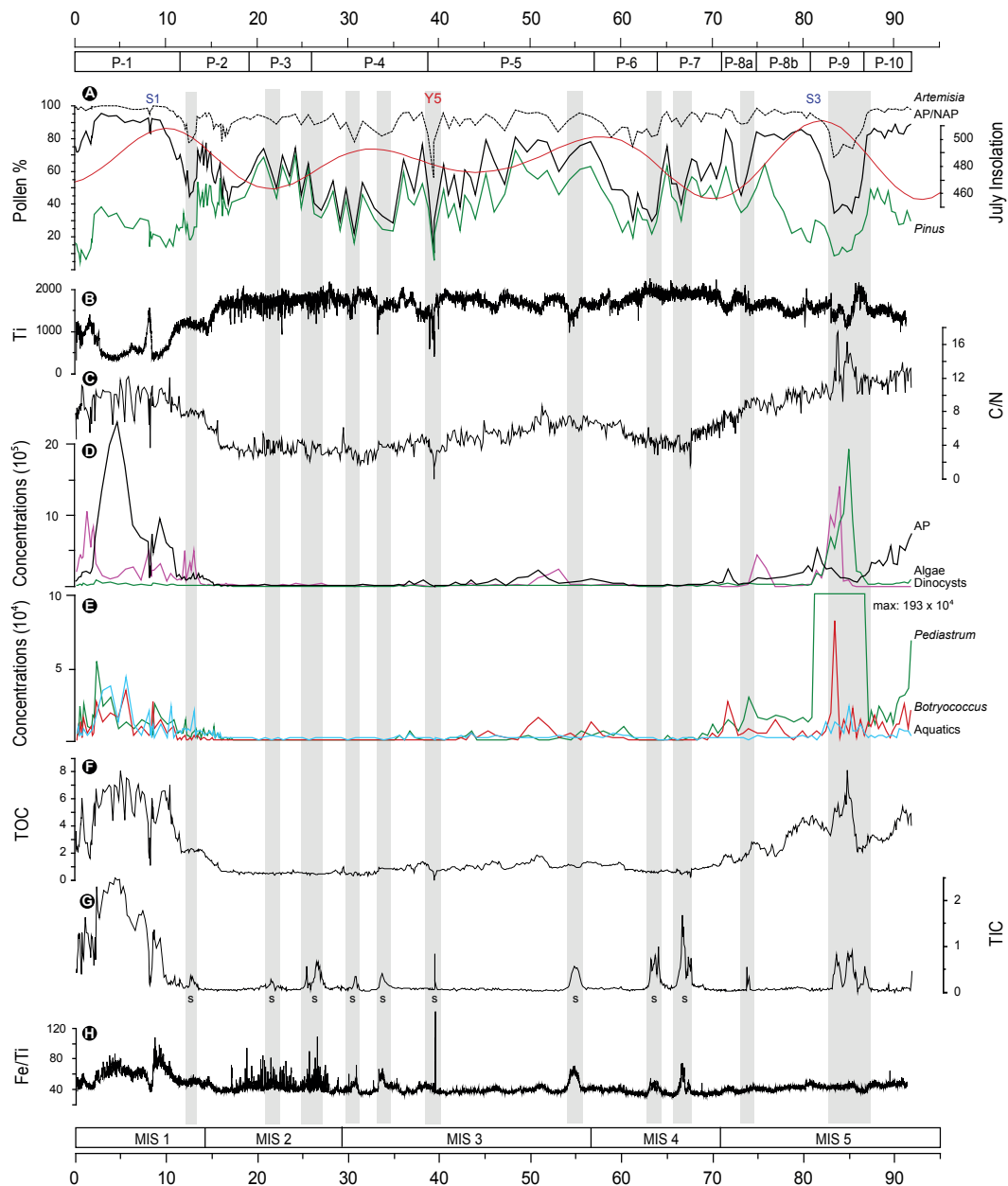| PAZ (cm, ka cal BP)	Lithology and geochemistry	Palynomorphs (percentages and concentrations)	Inferred paleo-environment
P-1 (204–0 cm, c. 11.5–Present)	high and fluctuating C/N, TOC, TIC and Fe/Ti (calcite); low Ti	AP > 67 % (mean 82 %); high AP conc. (mean 550×10^3 grains cm^{-3}); Mediterranean sclerophyllous taxa (*Phillyrea*, *Pistacia*, *Olea*) continuous curves; expansion of thermophilous deciduous trees (mostly *Quercus*); *Abies, Carpinus, Corylus, Fraxinus, Tilia, Fagus* maxima (> 10 %); aquatics and phytoplankton conc. peaks	closed evergreen, deciduous and mixed forests with thermophilous and sclerophyllous species; high lake productivity
P-2 (364–204 cm, c. 19–11.5) P-2c (364–277 cm, c. 19–15)	increasing (decreasing) TOC and C/N (Ti and Fe/Ti); sporadic occurrence of IRD; irregular laminations	AP < 78 % (mean 57 %); relatively high AP conc. (mean 69.5×10^3 grains cm^{-3}); gradual expansion of AP conc. and deciduous AP % (mostly *Quercus* and *Betula*), *Artemisia* and Chenopodiaceae peaks in P-2c and P-2a. Aquatic % maximum in P-2c.	transitional open vegetation with scattered pine and oak stands (including several other deciduous trees)
P-3 (525–364 cm, c. 26–19)	high (low) Ti (C/N, TOC); sporadic occurrence of IRD; irregular laminations; TIC and Fe/Ti peaks (siderite)	AP < 75 % (mean 62 %), *Pinus* dominates AP % (up to 70 %), *Quercus* % minimum (< 1 %); very low AP conc. (mean 13.5×10^3 grains cm^{-3}); increasing aquatic %	open steppe vegetation with scattered pine stands; low lake productivity
P-4 (760–525 cm, c. 39–26)	high (low) Ti (C/N, TOC); sporadic occurrence of IRD; irregular laminations; TIC and Fe/Ti peaks (siderite)	AP < 76 % (mean 50 %); low AP conc. (mean 22×10^3 grains cm^{-3}); Asteraceae peak (27 %), low (< 10 %) and declining *Quercus* %	open steppe vegetation with scattered pine stands; low lake productivity
P-5 (1027–760 cm, c. 57–39)	decreasing C/N and TOC; sporadic occurrence of IRD; TIC and Fe/Ti peaks (siderite)	AP < 80 % (mean 60 %); relatively high AP conc. (mean 64.5×10^3 grains cm^{-3}); *Pinus* dominates AP % (up to 60 %), *Quercus* (up to 19 %), continuous curves of other deciduous trees (e.g., *Carpinus, Ulmus*); max NAP % (90 %), conspicuous *Artemisia* spikes (up to 43 %); phytoplankton concentration peaks	transitional open vegetation with scattered pine and oak stands (including several other deciduous trees); increased lake productivity
P-6 (1180–1027 cm, c. 64–57)	increasing (decreasing) C/N and TOC (Ti); sporadic occurrence of IRD; TIC and Fe/Ti peaks (siderite)	AP < 65 % (mean 42 %); low AP conc. (mean 23.5×10^3 grains cm^{-3}); *Pinus* dominates AP % (up to 50 %), increasing *Quercus* % (up to 18 %); mean *Artemisia*, Chenopodiaceae and Poaceae % above 10 %; Poaceae peak (20 %); aquatics % peak (4.5 % mostly *Typha*)	open steppe vegetation with scattered pine and oak stands; low lake productivity
P-7 (1390–1180 cm, c. 71–64)	decreasing C/N and TOC; sporadic occurrence of IRD; TIC and Fe/Ti peaks (siderite)	AP < 75 % (mean 52 %); low AP conc. (mean 23.6×10^3 grains cm^{-3}); *Pinus* dominates AP % (up to 63 %), decreasing *Quercus* %; mean *Artemisia*, Asteraceae and Poaceae % above 10 %	open steppe vegetation with scattered pine and oak stands; low lake productivity
P-8 (1580–1390 cm, c. 81–71) P-8a (1480–1390 cm, c. 75–71) P-8b (1580–1480 cm, c. 81–75)	decreasing (increasing) C/N and TOC (Ti); in P-8a: sporadic occurrence of IRD, TIC peak (mussel horizon)	45 % < AP < 86 % (mean 76 %); relatively high AP conc. (mean 137×10^3 grains cm^{-3}); in P-8a: *Pinus* dominates AP % (up to 64 %), Poaceae max (19 %), phytoplankton concentration peak; in P-8b: maxima *Quercus* (34 %) and *Abies* (12 %)	transitional open vegetation with scattered pine and oak stands (including firs and several other deciduous trees)
P-9 (1680–1580 cm, c. 87–75)	C/N, TOC and TIC peaks; decreasing Ti	34 % < AP < 82 % (mean 51 %); relatively high AP conc. (mean 192×10^3 grains cm^{-3}); maxima *Betula* (10 %), *Artemisia* (32 %), Poaceae (17 %), Chenopodiaceae (12 %); phytoplankton conc. absolute maxima, first appearance of dinocysts and max (141×10^4 dinocysts cm^{-3})	transitional open vegetation with scattered oak and pine stands (including several other deciduous trees); high lake productivity
P-10 (1776–1680 cm, c. 92–87)	decreasing (increasing) C/N and TOC (Ti);	AP > 80 % (mean 85 %); high AP conc. (mean 444×10^3 grains cm^{-3}); *Pinus, Quercus, Abies, Carpinus* maxima (> 10 %); decreasing phytoplankton concentration	closed evergreen, deciduous and mixed forests; increased lake productivity

Fig. 5. Selected biological and geochemical proxies from Lake Prespa (core Co1215) plotted against age. **(A)** *Artemisia* (dashed line), AP/NAP (black), and *Pinus* (green) pollen percentages; mean July insolation at 40° N (W m^{-2}; red) computed in AnalySeries 2.0 (Paillard et al., 1996; data from Laskar et al., 2004); sapropels (S1, S3); and Y5 tephra layer. **(B)** Titanium (Ti) counts; **(C)** atomic C/N; **(D)** concentrations ($\times 10^5$) of arboreal pollen (AP; black), green algae (green) and dinoflagellates (purple); **(E)** concentrations ($\times 10^4$) of aquatics (blue), *Botryococcus* (red) and *Pediastrum* (green). Note the difference in scale, **(F)** total organic carbon (wt %); siderite (*s*) peaks are marked; **(G)** total inorganic carbon (wt %); **(H)** iron/titanium (Fe/Ti). Shaded intervals correspond to carbonate peaks precipitated at Lake Prespa during the last glacial.

Ti counts, which indicate fluctuating allochthonous clastic material input (i.e., Ti; Table 1, Fig. 5b and d). During the Holocene, the Prespa catchment underwent substantial changes in floristic composition as forests expanded (e.g., ascending treeline) and diversified (e.g., continuous presence of thermophilous species). The restricted erosion activity,

inferred from decreasing titanium counts, and maximum AP concentrations (absolute max of 23×10^5 grains cm^{-3}) suggest the closing of the tree canopy within the catchment. Besides the Holocene, the conspicuous absence or appearance of isolated grains of Mediterranean sclerophyllous

species over the last 92 ka suggests that (winter) temperatures were not favorable for their survival/expansion at Prespa.

Two periods (P-9 and P-8a) of rapid herb expansion interrupt forest continuity at the base of Co1215 (in MIS 5). The collapse of conifer populations, the relative stable *Quercus* and rising *Betula* percentages and pronounced peaks of *Artemisia* and Chenopodiaceae attest to increased aridity, dropping temperatures and a descending treeline in P-9 (c. 87–81 ka cal BP). A parallel AP concentration decrease supports the notion of thinning tree stands and forest retreat. A similar arboreal (mainly *Pinus*) response with maximum Poaceae (Fig. 4) percentages is evident in P-8a (c. 75–71 ka cal BP). In both zones, pollen spectra resemble the ones belonging to Younger Dryas (MIS 1; P-2a) discussed extensively elsewhere (Panagiotopoulos et al., 2013).

In contrast to the forested landscape inferred for MIS 5 and MIS 1, between P-7 and P-2c AP percentages stay on average below the 75 % boundary, suggesting these time periods represent a rather open landscape. As pollen percentages are dependent on each pollen type included in the pollen sum, some taxa such as *Pinus* with its exceptional pollen productivity and dispersal properties are over-represented in the relatively open landscapes encountered during full glacial conditions. These pollen zones, corresponding to MIS 4 (c. 71–57 ka cal BP; P-7 to partly P-6), MIS 3 (c. 57–29 ka cal BP; partly P-6 to partly P-4) and MIS 2 (c. 29–14 ka cal BP; partly P-4 to P-2c), contain relatively low arboreal pollen concentrations (on average below 65 000 grains cm^{-3}; Table 1, Fig. 5d) and have a high clastic content. The apparent opening of the landscape and/or lowering of treeline imply a climate regime with lower temperatures and a deficit in moisture required for tree growth within the catchment. Trees were restricted to favorable habitats provided by the diverse topography at Prespa. Arboreal relative percentages (reflecting mostly forest composition) were dominated by *Pinus* between MIS 4 and MIS 2. A prolonged phase of intermediate *Quercus* percentages occurs between P-6 and P-4, corresponding to MIS 3. Besides *Quercus*, continuous *Abies*, *Betula* and *Carpinus* curves along with intermittent presence of others (e.g., *Alnus*, *Corylus*, *Ulmus*, *Tilia*) suggest their survival most likely within the catchment. During this interval of abrupt AP percentage fluctuations, total tree abundance (percentages and concentrations) was high in comparison with the preceding (MIS 4) and ensuing (MIS 2) intervals (Table 1, Figs. 4 and 5d).

It is apparent that climate oscillations control the response of vegetation within the Prespa watershed, influencing spatial patterns and floristic composition through time. However, there are other environmental parameters, such as geomorphology, slope exposure, soil formation, lake level, pH and nutrient availability, which determine vegetation development in the terrestrial and aquatic ecosystems. Semi-aquatic and aquatic vascular plant pollen percentages in Prespa (Fig. 4) can be employed as a proxy to infer fluctuations in lake levels (e.g., Harrison and Digerfeldt, 1993). Poaceae

percentages are assumed to contain a portion of grassland (upland) and reed bed taxa (e.g., *Phragmites* sp.) growing at the littoral zone. In Co1215, Poaceae maxima are synchronous with *Artemisia* peaks (a proxy of increasing aridity) throughout the core. At first sight, this appears to be contradictory as grasslands usually expand with increasing precipitation. Hence, we assume that *Phragmites* sp. contribute a significant percentage to Poaceae expansions during these zones and consequently these abrupt expansions are estimated to be synchronous to fluctuating lake levels (e.g., in P-9 and P-8a; Fig. 4). Along with peaking *Typha* and Cyperaceae percentages, Poaceae percentages are used to infer intervals of spreading reed beds and sedgelands (e.g., in P-9, P-4, P-6, P-2c; Fig. 4). At this point, it should be underlined that changes inferred from aquatic pollen are relative and indicative of trends (e.g., a lowering of the lake level). They do not necessarily coincide with low or high stands of Lake Prespa (namely with actual water depth). In fact, the concomitant occurrence of *Nymphaea*, *Sparganium*, *Myriophyllum* and *Potamogeton* pollen suggest rather deep waters (> 6 m) at the coring site (Harrison and Digerfeldt, 1993) throughout the study period. Therefore, different lines of evidence (i.e., sedimentological, seismic, geochemical and isotopic data) are compiled to infer changes in the littoral and aquatic environment of Lake Prespa through time (see Sect. 5.1.2).

Green algae and dinoflagellate concentrations (Fig. 5d and e) are considered to represent periods when frequent phytoplankton blooms occurred. Rising temperatures and light intensity, nutrient availability, and the onset of lake stratification constitute the major parameters controlling (springtime) phytoplankton blooms (Wetzel, 2001). In mesotrophic and eutrophic lakes, diatoms and cyanobacteria (blue-green algae) account for dense blooms as a result of excess nutrient accumulation, notably phosphorus. On an annual basis, phytoplankton blooms are usually terminated with the gradual depletion of soluble nutrients (e.g., phosphorus, nitrogen, silicon) available for algae growth in the epilimnion (Wetzel, 2001). In Co1215, high plankton concentrations occur in MIS 5, MIS 3 and MIS 1. In general, these intervals coincide with increased forest cover, suggesting higher moisture availability and/or temperatures in the catchment. However, absolute maximum values occurred during a short interval in MIS 5 concurrent with an abrupt arboreal retreat (P-9). Matzinger et al. (2006) discussed the dramatic impact of changes in lake volume on the concentration of dissolved nutrients (in particular phosphorus), considering the relatively shallow depth of Lake Prespa with respect to its surface area. In the presence of low lake levels, increased wave and current activity and thus enhanced mixing and oxygenation are expected. In addition, increased nutrients (e.g., phosphorus) and oxygenation could lead to high lake productivity and extensive blooms.

The lake productivity proxies in Co1215 (Figs. 4 and 5d and e) comprise green algae (*Pediastrum* and *Botryococcus* species), dinoflagellates (*Gonyalux*-type) and aquatic

vascular plants (emerged, submerged and floating; Fig. 4). Along with terrestrial pollen (Fig. 5a and d), they are assumed to indicate changes in organic matter (OM) sources within the Prespa catchment. Atomic C/N values between 4 and 10 imply that sedimentary OM in Co1215 originated from non-vascular plants and are probably affected by decomposition (Meyers, 1994). The synchronous C/N, TOC, AP/NAP and plankton fluctuations (Fig. 5a, c and f) downcore and peaking C/N values corresponding to forested intervals (i.e., MIS 5 and MIS 1) suggest that diagenesis did not alter significantly the source signal of OM for the past 92 ka. Indeed, Rock–Eval analysis of the Prespa sediments confirmed that although oxidation did play an active role, the source of OM was found to be a function of climate/hydrology (Leng et al., 2013). High rates of OM oxidation are mostly found during MIS 4 and MIS 2 and coincide with phases of open catchment vegetation, low primary production and siderite precipitation in the lake sediments (Leng et al., 2013).

Carbonate minerals formed intermittently in Lake Prespa throughout the period examined (Fig. 5g). Calcite precipitation occurred sporadically in MIS 5 and continuously in MIS 1 (Holocene). In most cases, carbonate precipitation is dominated either by evaporative concentration or by the supply of calcium ions (in highly alkaline systems). Increases in temperature (or salinity) may also cause the removal of CO_2 through lowered solubility and calcite precipitation. Calcite precipitation is often triggered by pH shifts induced by photosynthesis (higher pH and removal of carbon dioxide causing precipitation) (Cohen, 2003). Dean (1999) argued that although eutrophication may increase the pH and promote calcite precipitation, subsequent respiration and decomposition of OM in the hypolimnion lower the pH releasing CO_2 and thus promote $CaCO_3$ dissolution. As a result, most of the autochthonous precipitated calcite is dissolved in the anoxic and more acidic hypolimnion (Dean, 1999; Cohen, 2003). Dittrich and Koschel (2002) have shown that sedimentation of phosphorus and calcite precipitation are closely linked, and that artificial addition of $Ca(OH)_2$ in the hypolimnion during summer in a stratified hard-water lake intensified calcite precipitation and lowered the trophic state, enhancing the internal phosphorus sink. The absence of calcium carbonate in the last glacial is assumed to be a result of low trophic status, dissolution due to aerobic decomposition of organic matter and inhibited ion supply from the catchment (Aufgebauer et al., 2012). Isotopic data (both $\delta^{13}C_{org}$ and $\delta^{13}C_{TIC}$) from Co1215 suggest that during the last glacial carbon input was limited, most likely due to more limited recharge of soil-CO_2 leached from the catchment, while in the Holocene a greater supply of soil-derived CO_2 is inferred (Leng et al., 2013). Well-developed soils during the Holocene are also inferred from increased forest cover and tree species diversity registered in the pollen record (Panagiotopoulos et al., 2013). However, TIC ($FeCO_3$) peaks in Co1215 are scattered within the last glacial. The TIC peaks throughout MIS 4 to MIS 2

occur alongside Fe peaks and suggest changing redox conditions and burial processes, such as proposed for peaks in Mn (Wagner et al. 2010).

Calcite precipitation during MIS 5 is mostly confined to a short interval between 87–82 ka cal BP and two isolated peaks at 91 and 74 ka cal BP. High and fluctuating TOC throughout MIS 5 implies high catchment productivity (Fig. 5f). The apparent decoupling of organic and inorganic carbon preserved in Lake Prespa sediments points to increased accumulation and/or deposition of organic matter and intensified dissolution, respectively (Fig. 5f and g). The first TIC peak at the base of Co1215 is the only interval in MIS 5 coincident with a forested watershed phase (high AP percentages and concentrations) and relatively high green algae content (*Pediastrum*), suggesting high temperatures, limited decomposition and seasonal bottom water anoxia (Fig. 5a and d). Between 87 and 82 ka cal BP, three distinct TIC (calcite) peaks are expressed concurrently in fluctuating C/N and TOC. However, the TIC peaks between 87–82 and 74 ka cal BP occur during periods of declining tree cover and apparently lower lake levels. In line with MIS 5, Holocene sediments with high TOC content suggest high primary production in the Prespa watershed, as well as enhanced deposition of OM, and thus seasonal stratification and hypolimnion anoxia. Relatively high phytoplankton (green algae and dinoflagellates) concentrations during this interval imply increased nutrient accumulation and/or higher temperatures. This increase in lake productivity was coincident with forest expansion (P-1 in Fig. 4) and decreasing allochthonous input (Fig. 5b). High and synchronous TIC content was attributed to authigenic calcite precipitation, corresponding to higher temperatures and productivity in the lake (Aufgebauer et al., 2012). However, during the early Holocene TIC values (Fig. 5g) remained low, implying that increased dissolution of calcium carbonates occurred with seasonal stratification. In MIS 4, the declining TOC, C/N ratio and retreating catchment vegetation suggest limited carbon input from the catchment as well as increased degradation of OM due to enhanced mixing promoted by a colder climate and/or a lower lake level. The synchronous *Typha* and Poaceae maxima at the top of P-6 point to a lake level lowering (Fig. 4). Two pronounced TIC peaks concomitant to Fe/Ti peaks (Fig. 5g and h) indicate changes in the redox front conditions and correspond to distinct minima in AP percentages (at 66 and 63 ka cal BP). In MIS 3, relatively high C/N values (above 6) up to c. 50 ka cal BP imply an increased input of terrestrial OM and/or inhibited decomposition. From c. 40 ka cal BP till the end of MIS 2, the geochemical proxies and the AP percentages show abrupt fluctuations. The TIC peaks are concurrent with AP percentage minima, as well as increased and fluctuating Fe/Ti, suggesting abrupt shifts in temperatures, moisture availability, mixing regime and redox conditions. The low TOC and C/N values (below 6) during this period suggest that primary productivity declined and/or decomposition of OM increased. In addition, the very low

phytoplankton concentrations point to restricting temperatures and/or nutrient availability for their growth.

5.1.2 Understanding ecological processes, triggers and thresholds

Three noteworthy events involving lentic organisms are encountered in the Prespa sequence (phytoplankton blooms, dinoflagellate migration and formation of a shell horizon) and their potential ecological-indicator value is assessed.

The *Pediastrum* and subsequent dinoflagellate peaks at 85 ka and 84 ka cal BP (1648 and 1624 cm) are the only recorded incidents of planktonic population expansion of this order (maxima of 19×10^5 coenobia cm^{-3} and 14×10^5 dinoflagellates cm^{-3}, respectively). TIC peaks (calcite) between 87 and 82 ka cal BP, an abrupt opening of the landscape (AP, Ti) and peaking macrophyte (e.g., *Typha* and Cyperaceae) and plankton percentages suggest that the catchment underwent dramatic changes within this interval. The descending treeline left large areas of the surrounding limestone slopes barren and exposed to chemical weathering and erosion. Rising percentages of emergent aquatic vegetation point to fluctuating lake levels and frequent flooding of the littoral zone. Increased aridity and lower annual temperatures inferred from corresponding pollen spectra suggest that these flooding events can be related to seasonal releases of snowmelt from local ice caps (Woodward and Hughes, 2011). Owing to bedrock composition of the Prespa catchment, lake water likely became supersaturated with respect to calcium during these events. Pronounced calcium peaks concurrent with TIC peaks back this interpretation. Moreover, relative high fine-sand content (up to 14 vol % at 1578 cm) corroborates the notion of increased wave and current activity, indicating lowering lake levels and/or increased aeolian activity. Therefore, the expansion of sedgelands (Cyperaceae) and reed beds (e.g., *Phragmites* and *Typha*) attest to lower lake levels and most likely also accounted for increasing OM accumulation allowing riparian trees (i.e., *Salix* and *Alnus*) to reclaim land and in effect pushing the reed beds further into the lake. It should also be noted that during this period summer insolation and light intensity were increasing (Fig. 5a; Laskar et al., 2004). This could imply that aridity promoted by enhanced seasonality (rather than lower temperatures) was the decisive parameter controlling the aforementioned environmental response. However, the conspicuous absence of Mediterranean taxa pollen points to a rather dry and cold climate regime similar to the one inferred during the late glacial to Holocene transition (Panagiotopoulos et al., 2013).

The acceleration of calcium ion accumulation and generally enriched nutrient concentrations caused by a presumed lower stand of Lake Prespa provided ideal conditions for algal growth (see Sect. 5.1.1). The unprecedented phytoplankton blooms (inferred by peaking *Pediastrum* and dinoflagellate concentrations) were in turn instrumental in

triggering the formation of calcite (nucleation) and thus catalyzed its precipitation. The concomitant double TOC peak and low terrestrial productivity suggest that phytoplankton was the major source of OM deposited. Atomic C/N values greater than 10 suggest allochthonous input (OM originating from vascular plants; Meyers, 1994). Considering that both planktonic species preserved in pollen slides are composed of robust sporopollenin and cellulose (for green algae and dinoflagellates respectively), the relative high C/N ratio (above 12) can be partly attributed to these properties and likely due to restricted decomposition of OM. The increase in macrophyte percentages suggests increased macrophyte biomass (i.e., OM of vascular plant origin; Fig. 5e) within this interval, which probably accounted for the high C/N ratio as terrestrial biomass retreated substantially (low terrestrial pollen percentages and concentrations). Indeed, relatively high macrophyte percentages (e.g., *Typha*, Cyperaceae and *Sparganium*) and concentrations are registered between c. 87–81 ka cal BP (P-9; Fig. 4).

In contrast to green algae, dinoflagellates are not found in the period prior to 87 ka cal BP (1672 cm). Thus, it is postulated that they were most likely introduced (reintroduced?) into the lake by migrating (avian) fauna. In fact, Wilke et al. (2010) reported the appearance of bivalves (*Dreissena* spp.) in artificial water reservoirs constructed during the last decades in Greece, implying the occurrence of such re/introduction events on a regular basis. The third event accounts for the TIC peak (calcite) at 74 ka cal BP comprising a horizon of *Dreissena* (*presbensis*) fragments and was tentatively attributed to low lake levels (Wagner et al., 2012).

A *Dreissena* shell layer (1463–1458 cm) formed at 74 ka cal BP and corresponds to the last calcite peak in MIS 5. *Dreissena* spp. are native to several Balkan lakes (Albrecht et al., 2007) and in contrast to their infamous relative, namely the invasive zebra mussel (*D. polymorpha*), form an integral and vital link in the trophic chain of these ecosystems. These freshwater bivalves exhibit a similar feeding strategy to their marine counterparts (i.e., filtering particles suspended in the water column) and preferably attach to solid substrates (Griffiths et al., 2004). Sparse *Dreissena* fragments were also encountered and dated in the uppermost centimeters of Co1215. Considering the current water depth and distance to the shore, these fragments were most likely transferred to the coring location with waves and currents. A similar transfer mechanism and lower lake levels can be invoked to explain the formation of the mollusk horizon. Wagner et al. (2012) interpreted the undulating reflections found in hydroacoustic profiles from Lake Prespa during this interval as the result of intensified wave/current activity and low lake levels. Accordingly, the opening of catchment vegetation and decreasing percentages of deciduous trees in P-8a (c. 75–71 ka cal BP) point to a moisture deficit and dropping temperatures. In general, aquatic vegetation abundance is rather low with the exception of a pronounced Poaceae maximum, which could indicate a high *Phragmites* percentage

(see Sect. 5.1.1). In addition, measured phytoplankton concentrations are peaking within this zone (P-8a). It seems plausible that the expansion of the littoral zone caused by a lake level lowering is responsible for the population growth of *Dreissena*, providing suitable habitats and nourishment. Based on genetic and mismatch analyses, Wilke et al. (2010) modeled the spatial and demographic expansion of *Dreissena* at Prespa and reported estimated ages of 72 and 113 ka for these expansions, respectively. It can be argued that demographic expansion of *D. presbensis* at Prespa is related to the unprecedented event of 74 ka cal BP, marking the end of MIS 5.

5.2 Comparison with regional and global records

5.2.1 Mediterranean records

On a regional scale, the Prespa pollen record is probably best compared to the Italian Monticchio (Allen et al., 1999) and Greek Ioannina (Tzedakis et al., 2002) pollen archives (Fig. 6), as both records have a similar climate (sub-Mediterranean), elevation (middle-altitude, located at 656 and 470 m a.s.l., respectively), sedimentation regime (absence of hiatus), sample resolution (detecting millennial-scale variability), and timescale (reaching back to MIS 5). Despite the differences in elevation, topography, sedimentation, chronology and plant composition, some general conclusions can be drawn from the comparison between the three pollen records. It should be noted that the Monticchio sequence features an independent chronology based on tephrostratigraphy and varve counting. Orbital tuning was applied beyond the range of radiocarbon dating in core I-284 (Ioannina), which differs from the tuning procedure for the basal part of Co1215. As evidenced in Sect. 5.1, pollen relative percentages can be misleading in respect to the actual forest coverage of the examined paleo-landscapes. Consequently, the ensuing discussion focuses on prominent features that can be traced across several proxies and/or archives.

Further regional records include the oxygen stable isotopes measured in speleothems from Soreq Cave (Bar-Matthews et al., 2000, 2003) and the alkenone-derived SST curve from core MD01-2444 at the Iberian margin (Martrat et al., 2007).

The temperate tree (AP − *Juniperus* + *Pinus*, mostly *Quercus*) curve of Ioannina (Fig. 6d), the site with the lowest altitude, resembles the AP curves of Prespa and Monticchio. This is partly due to the rather limited role of *Pinus* at the Ioannina basin and the dominance of deciduous *Quercus* in the pollen spectra (Tzedakis et al., 2002). A similar picture emerges from Monticchio (Allen et al., 2000), where *Pinus* relative abundance is limited and attains maximum values only around the LGM (> 40 %) while *Quercus* percentages dominate pollen spectra (i.e., MIS 5, MIS 3 and

MIS 1). In comparison, core Co1215 has the highest (lowest) *Pinus* (*Quercus*) percentages.

Among other factors, it has been suggested that mid-altitude sites were better suited in sustaining refugial temperate tree populations due to the effect of orographic precipitation (Bennett et al., 1991). Tzedakis et al. (2004) studied three pollen records from contrasting bioclimatic areas in Greece and demonstrated the importance of local topography and ecological thresholds in controlling the response of the vegetation to climate variability. The Lake Prespa catchment sustained temperate tree populations throughout the last glacial (Fig. 4). However, the intermittent appearance and very low values of some drought-sensitive taxa, such as *Fagus*, *Ulmus* and *Tilia*, during MIS 4 to MIS 2 imply that environmental conditions were challenging for growth at an altitude of 849 m a.s.l. (minimum). Taking into account the individual characteristics of each record examined here, it can be argued that the Lake Prespa catchment at 849 m a.s.l. seems to form roughly the upper distribution limit of drought-sensitive trees at these latitudes in Mediterranean mountains.

The *Quercus* curve of Co1215, although continuous, registers very low oak values, in particular in MIS 4 and MIS 2 (Fig. 6f). These intervals show the maximum contraction of *Quercus* percentages in all three pollen records, suggesting cold and dry conditions and a rather open landscape (Fig. 5d). The $\delta^{18}O$ record from Israel is in agreement with pollen records and depicts pluvial conditions in MIS 5 and MIS 1 (Fig. 6c). As precipitation in that area originated from the Mediterranean Sea (Bar-Matthews et al., 2003), and given its independent ^{230}Th-U dating, it appears that the conditions described above were synchronously prevalent across the (central and eastern) Mediterranean.

The deposition of two Sapropel layers (S3 and S1) in the eastern Mediterranean coincided with peaks in the speleothem oxygen-isotope record and AP percentage maxima in all pollen records (implying a notable increase in rainfall). It was originally proposed that these organic rich layers, which formed under anoxic conditions in the eastern Mediterranean basin, originated during periods of increased Nile River runoff fed by enhanced monsoon intensity (Rossignol-Strick, 1985). It was demonstrated that increased Nile discharge was not the exclusive cause of sapropel formation (Rohling and Hilgen, 1991). However, Rossignol-Strick (1985) first described the temporal connection between sapropel formation and orbital forcing. Hilgen (1991) correlated sapropels to precession minima (when perihelion occurs in boreal summer and aphelion in boreal winter) and eccentricity maxima. With this orbital configuration, the seasonal insolation contrast (enhanced summer and subdued winter insolation) is greater and thus it affects atmospheric and oceanic circulation (e.g., monsoonal intensification). At Prespa, increased lake and catchment primary production are associated with June insolation maxima during MIS 5, MIS 3 and MIS 1 (Fig. 5). AP percentage maxima concurrent with
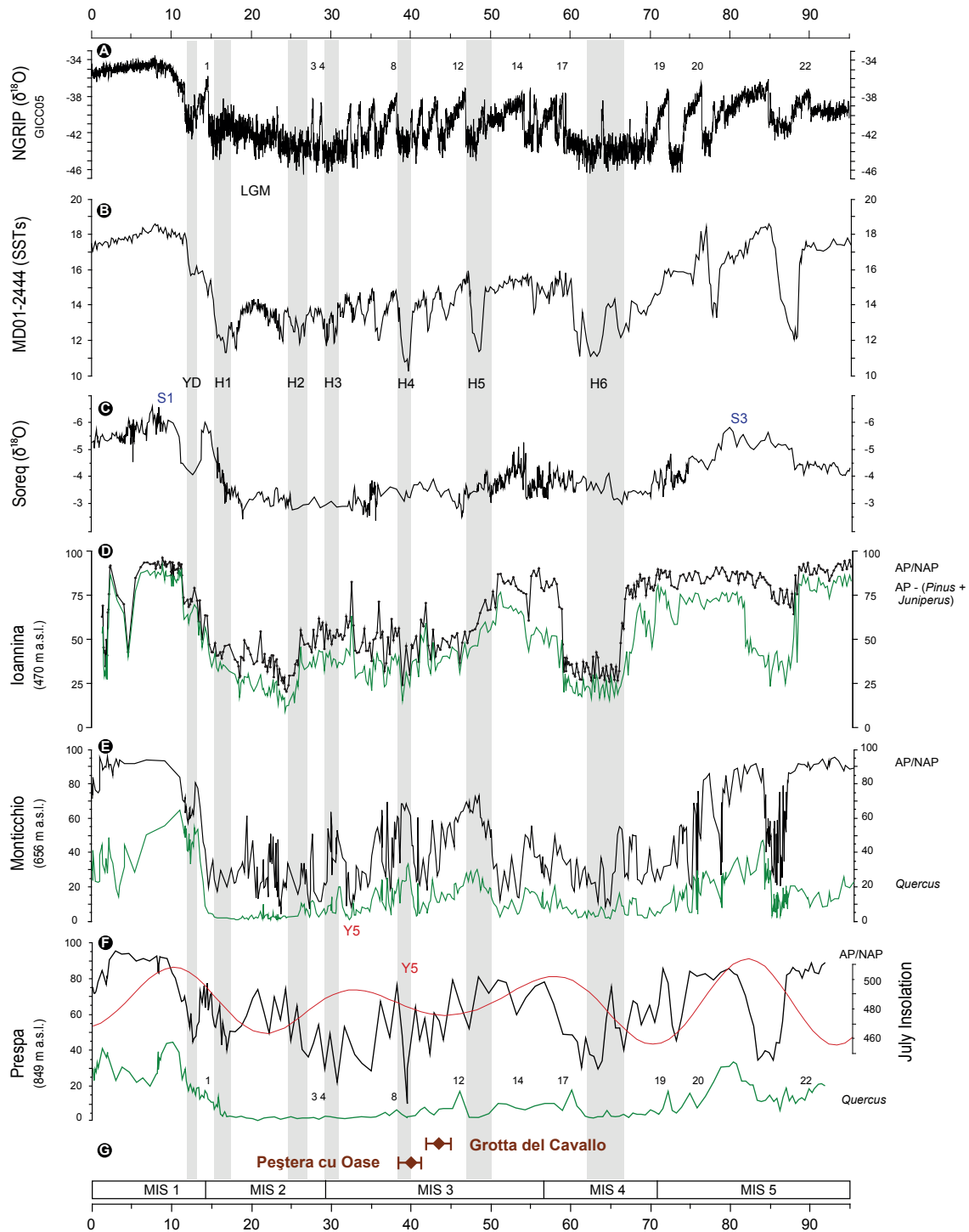
Fig. 6. Comparison of Prespa proxies with regional and global records. **(A)** Ice core oxygen isotopes (‰) measured in NGRIP (GICC05 modelext) with Dansgaard–Oeschger (D–O) warming events/Greenland interstadials (GI) numbered; Last Glacial Maximum is indicated; **(B)** alkenone derived ($U_{37}^{k'}$) sea surface temperatures (SSTs) measured in core MD01-2444 from the Atlantic Ocean; **(C)** oxygen isotopes (‰) measured in speleothems from Soreq Cave (Israel) and sapropel depositions (S1, S2) in the eastern Mediterranean Sea; **(D)** AP/NAP (black) and AP minus *Pinus* and *Juniperus* (green) pollen percentages in I-284 from Lake Ioannina (Greece); **(E)** AP/NAP (black) and *Quercus* (green) pollen percentages from Lago Grande di Monticchio (Italy); **(F)** AP/NAP (black) and *Quercus* (green) pollen percentages from Lake Prespa, mean July insolation at 40° N (W m^{-2}; red); **(G)** calibrated radiocarbon ages from neighboring sites with modern human remains. Gray bars correspond to Heinrich events in MD01-2444.

sapropel deposition are preceded by pronounced retractions (GS 22 and YD) of trees evident in all records presented.

5.2.2 Global records

Millennial-scale climate variability was expressed in the North Atlantic during the last glacial at a suborbital scale. Short-lived climate oscillations, such as Heinrich events and Dansgaard–Oeschger (D–O) cycles, have been detected in different proxies in the marine as well as in the terrestrial realm (Dansgaard et al., 1984; Heinrich, 1988; Bond et al., 1993). Marine cores from the Iberian continental margin have been instrumental in establishing the link between ice and other terrestrial records showing the synchronous response of European vegetation to Greenland climate oscillations (Cacho et al., 1999; Sánchez Goñi et al., 2000). Allen et al. (1999) associated millennial-scale variability at Monticchio with the one observed in Greenland ice cores and argued that the Mediterranean region responded to changes in North Atlantic climate rapidly. At Ioannina, Tzedakis et al. (2002) suggested that AP absolute minima should correlate to Heinrich events recorded in marine cores from the Iberian margin.

At Prespa, Wagner et al. (2010) correlated peaks in Mn and Zr/Ti from cores Co1202 and Co1204 (retrieved from Prespa and Ohrid, respectively; Fig. 2) with cold intervals associated with Heinrich events in the North Atlantic. Sediments of the longest core from Lake Prespa to date (Co1215) react sensitively to suborbital climate oscillations and capture these global signals in different proxies. Synchronous peaks in Fe and TIC correlate well with H6, H4, H3, and H2, but they are absent during H5 and H1, implying the complex interplay between climate and environmental parameters and limnological processes. Despite the resolution constraints, the *Quercus* curve picks up several D–O warming events (Fig. 6f), while Heinrich events are imprinted as distinct minima in AP percentages. Heinrich event 4, which is concurrent with the deposition of the Y5 tephra layer (Campanian Ignimbrite; de Vivo et al., 2001; Lowe et al., 2012), had the greatest impact (AP percentages absolute minimum) on the vegetation at the Lake Prespa catchment. This observation is in agreement with the SST record from the Iberian margin (Fig. 6b), which was associated with the lowest sea surface temperatures ($\sim 10\,^\circ$C) within the period studied. Consequently, the Campanian Ignimbrite eruption was not solely responsible for the conditions experienced downwind, but probably enhanced the impacts experienced by local ecosystems. The combined effect of H4 and the volcanic ash also affected the other two pollen sites, as registered by significant declines of AP percentages.

5.3 Environmental constraints posed on hominid populations

Modern human colonization of Europe is in the spotlight for researchers from a variety of disciplines. Genetic studies (involving mitochondrial and Y-chromosome DNA) confirmed the African origin of modern humans and estimated their dispersal out of the continent between c. 80 and 60 ka BP (Mellars, 2006). Although skeletal remains from Skhul and Qafzeh caves in Israel indicate an early and apparently short-lived colonization of the Levant in MIS 5 (c. 100 ka BP), there are no signs of dispersal at such an early stage into Europe (Mellars, 2011; Richter et al., 2012).

The Aurignacian technocomplex, associated with many distinctive features of "modern" cultural behavior, took place at c. 40 ka (Upper Paleolithic), according to the archaeological record and has been traditionally linked with the dispersal of modern humans into Europe (Mellars, 2011; Richter et al., 2012). This period differs considerably from the preceding Middle Paleolithic, which is considered to be formed of Neanderthal communities (Mellars, 2011). Mellars (2004) pointed out that major constraints in the process of unraveling these migration trajectories have been the quality of dated material and the implicit limitations of radiocarbon dating and calibration techniques at the time. Despite the continuous advances in ^{14}C calibration (Reimer et al., 2009), the selection and treatment of dated material (e.g., shell, bone) is critical and can bias the acquired ages.

One well-established migration route for subsequent modern human dispersals westwards into Europe is considered to be the Danube River valley (Conard, 2002; Conard and Bolus, 2003; Mellars, 2004; Zilhão et al., 2007). The Peștera cu Oase site located in close proximity to the Danube in the southwestern Carpathians (Fig. 1) yielded one of the oldest directly dated human finds in the Balkans with an age of c. 40 ka cal BP (Trinkhaus et al., 2003; Zilhão et al., 2007). Recent evidence from a site in the United Kingdom (Higham et al., 2011) provided estimates of a human maxilla with an age of c. 43 ka cal BP, making it the oldest known modern human fossil in northwestern Europe to date. Assuming that one of the primary dispersal routes crossed the Balkan Peninsula, it should be expected that modern human finds in this and surrounding areas should be at least of the same age. Indeed, deciduous molars of modern human origin from Grotta del Cavallo (associated with the Uluzzian industry) were dated indirectly at c. 44 ka cal BP (Benazzi et al., 2011). The only known sites associated with this technology outside of the Italian peninsula are located in the Peloponnese, Greece (layer V at Klissoura, Cave 1; Koumouzelis et al., 2001; Lowe et al., 2012), and consequently a Levantine origin can be assumed (Mellars, 2011), although the Uluzzian is absent in the Near East.

The pollen record from Lake Prespa reveals a period of relative high AP and *Quercus* percentages between 60 and 35 ka cal BP, which are interpreted as the signature

of increased precipitation and higher temperatures (Fig. 6g). The oxygen isotope record from Israel registers a concurrent increase in precipitation at the Levant that coincides with the onset of MIS 3 (Fig. 6c). These findings, apparent in regional and global archives, suggest that climatic conditions were favorable for sustained forest growth within this interval at Prespa. Müller et al. (2011) argued that the summer insolation maximum at c. 58 ka cal BP resulted in a northward displacement of the Intertropical Convergence Zone (associated with increased rainfall in northern Africa) and thus facilitated modern human dispersal out of the continent during the period between 55 to 50 ka cal BP (GI 14-13). Based on a collapse of AP percentages at the Tenaghi Philippon record concurrent with Heinrich event 5 (Fig. 6b), the authors suggested that modern human populations entered Europe, taking advantage of the demographic vacuum left by retreating Neanderthals during this centennial event.

The impact of the H5 event (c. 48 ka cal BP) at Prespa, as is the case for Ioannina, was apparently less severe on arboreal vegetation, given the dating and sampling constraints. As a consequence, the climatic and environmental conditions across the southwestern part of the Balkan Peninsula remained favorable for modern human occupation during most of the MIS 3. A precipitation gradient between western and eastern Greece exists today and was present during the last glacial, as was demonstrated in pollen archives from Greece (Tzedakis et al., 2004). Differences in local parameters, such as topography and plant composition, can therefore hamper the comparison between different records and proxies (even within similar climate regimes). Thus, the need of a dense network of paleo-records from a region is critical for the accurate reconstruction of climatic and environmental conditions along potential corridors of human migration.

It should also be noted that ice accumulation during glacial times was a major factor in shaping coastal planes and determining the paleo-coastline (Waelbroeck et al., 2002). Sea level fluctuations (of up to 100 m, see the 100 m contour line marked in Fig. 1) were reconstructed during MIS 3, exposing large areas of the continental shelf during the last glacial period (Siddall et al., 2003). In most certainty, several of these were used for the dispersal of our ancestors into Europe (e.g., Tourloukis and Karkanas, 2012).

6   Conclusions

The late glacial pollen record of Co1215 hints to the refugial character of the Prespa watershed during the last glacial period (Panagiotopoulos et al., 2013). This study confirms the survival of several deciduous temperate trees in the catchment since MIS 5. At an altitude of 849 m a.s.l., the study area most likely formed the upper limit of their glacial distribution at these latitudes within the Mediterranean region. The middle altitude, the diverse topography and the relative

proximity to the Adriatic Sea were decisive factors in shaping Prespa's microclimate throughout this interval.

These topographical characteristics in concert with the relative shallow morphology of Lake Prespa enabled the registration of centennial- to millennial-scale climate oscillations. The ecosystems of Lake Prespa and its watershed respond sensitively to D–O cycles and Heinrich events occurring in the North Atlantic and propagated into the Mediterranean through atmospheric and ocean circulation. Our multi-proxy approach captures the imprint of climatic signals in biotic as well as abiotic components of the local environment.

Three major phases of vegetation development, closely following climate variability, are distinguished for the last 92 ka cal BP. The wooded phases of MIS 5 and MIS 1 dominated by deciduous trees with higher temperatures and moisture availability, the rather open but wooded landscape with significant temperate-tree presence of MIS 3 and the pine-dominated wooded-steppe (open landscape) of MIS 4 and MIS 2 when temperatures and moisture availability declined. The succession of the forest density in the catchment is also depicted in the geochemical parameters, such as the titanium and total organic carbon curves, which follow closely the landscape evolution. Periods of reduced forest cover or a declining treeline (MIS 4 and MIS 2) resulted in enhanced erosional activity in the catchment and restricted lake productivity. Siderite formation occurs sporadically throughout the last glacial and signified substantial changes in lake mixing and redox conditions. Several of these peaks depicted in the TIC curve are concurrent with short-lived cold events and probably represent far field responses to the North Atlantic events. During periods of enhanced lake productivity (MIS 5 and MIS 1), calcite is precipitated in the lake and the lake-mixing regime is altered.

The Lake Prespa record appears to be in good agreement with regional and global archives, depicting orbital and sub-orbital climate variability. Despite the limitations of the age model of Co1215 (i.e., tuning with NGRIP curve at the basal part), major climate events are in phase with other archives in the eastern Mediterranean featuring independent chronologies (e.g., speleothem records; Bar-Matthews et al., 2000, 2003). The Prespa record as well as other reference archives from the Mediterranean point to a time window encompassing MIS 3 when the climate conditions were likely favorable for modern human dispersal from the Levant into Europe.

References

Albrecht, C., Schultheiß, R., Kevrekidis, T., Streit, B., and Wilke, T.: Invaders or endemics? Molecular phylogenetics, biogeography and systematics of Dreissena in the Balkans, Freshwater Biol., 52, 1525–1536, doi:10.1111/fwb.2007.52.issue-8, 2007.

Allen, J. R. M., Brandt, U., Brauer, A., Hubberten, H. W., and Huntley, B.: Rapid environmental changes in southern Europe during the last glacial period, Nature, 400, 740–743, 1999.

Allen, J. R. M., Watts, W. A., and Huntley, B.: Weichselian palynostratigraphy, palaeovegetation and palaeoenvironment; the record from Lago Grande di Monticchio, southern Italy, Quatern. Int., 73/74, 91–110, 2000.

Aufgebauer, A., Panagiotopoulos, K., Wagner, B., Schaebitz, F., Viehberg, F. A., Vogel, H., Zanchetta, G., Sulpizio, R., Leng, M. J., and Damaschke, M.: Climate and environmental change in the Balkans over the last 17 ka recorded in sediments from Lake Prespa (Albania/F.Y.R. of Macedonia/Greece), Quatern. Int., 274, 122–135, doi:10.1016/j.quaint.2012.02.015, 2012.

Bar-Matthews, M., Ayalon, A., and Kaufman, A.: Timing and hydrological conditions of Sapropel events in the Eastern Mediterranean, as evident from speleothems, Soreq cave, Israel, Chem. Geol., 169, 145–156, 2000.

Bar-Matthews, M., Ayalon, A., Gilmour, M., Matthews, A., and Hawkesworth, C. J.: Sea-land oxygen isotopic relationships from planktonic foraminifera and speleothems in the Eastern Mediterranean region and their implication for paleorainfall during interglacial intervals, Geochim. Cosmochim. Acta, 67, 3181–3199, 2003.

Benazzi, S., Douka, K., Fornai, C., Bauer, C. C., Kullmer, O., Svoboda, J., Pap, I., Mallegni, F., Bayle, P., Coquerelle, M., Condemi, S., Ronchitelli, A., Harvati, K., and Weber, G. W.: Early dispersal of modern humans in Europe and implications for Neanderthal behaviour, Nature, 479, 525–528, doi:10.1038/nature10617, 2011.

Bennett, K. D., Tzedakis, P. C., and Willis, K. J.: Quaternary refugia of north European trees, J. Biogeogr., 18, 103–115, 1991.

Blondel, J., Aronson, J., Bodiou, J.-Y., and Boef, G.: The Mediterranean Region. Biological Diversity in Space and Time, Second Edition, Oxford University Press, Oxford, 2010.

Bond, G., Broecker, W., Johnsen, S., McManus, J., Labeyrie, L., Jouzel, J., and Bonani, G.: Correlations between climate records from North Atlantic sediments and Greenland ice, Nature, 365, 143–147, 1993.

Cacho, I., Grimalt, J. O., Pelejero, C., Canals, M., Sierro, F. J., Flores, J. A., and Shackleton, N.: Dansgaard–Oeschger and Heinrich event imprints in Alboran Sea paleotemperatures, Paleoceanography, 14, 698–705, 1999.

Cohen, A. S.: Paleolimnology, The History and Evolution of Lake Ecosystems, Oxford University Press, Oxford, 500 pp., 2003.

Conard, N. J.: The timing of cultural innovations and the dispersal of modern humans in Europe, Terra nostra, 2002/6, 82–94, 2002.

Conard, N. J. and Bolus, M.: Radiocarbon dating the appearance of modern humans and timing of cultural innovations in Europe: new results and new challenges, J. Hum. Evol., 44, 331–371, doi:10.1016/S0047-2484(02)00202-6, 2003.

Damaschke, M., Sulpizio, R., Zanchetta, G., Wagner, B., Böhm, A., Nowaczyk, N., Rethemeyer, J., and Hilgers, A.: Tephrostratigraphic studies on a sediment core from Lake Prespa in the Balkans, Clim. Past, 9, 267–287, doi:10.5194/cp-9-267-2013, 2013.

Dansgaard, W., Johnsen, S., Clausen, H. B., Dahl-Jensen, D., Gundestrup, N., Hammer, C. U., and Oeschger, H.: North Atlantic climatic oscillations revealed by deep Greenland ice cores, edited by: Hansen, J. E. and Takahashi, T., American Geophysical Union, Washington, D.C., 288–298, 1984.

Dean, W. E.: The carbon cycle and biogeochemical dynamics in lake sediments, J. Paleolimnol., 21, 375–393, 1999.

De Vivo, B., Rolandi, G., Gans, P. B., Calvert, A., Bohrson, W. A., Spera, F. J., and Belkin, H. E.: New constraints on the pyroclastic eruptive history of the Campanian volcanic Plain (Italy), Miner. Petrol., 73, 47–65, 2001.

Dittrich, M. and Koschel, R.: Interactions between calcite precipitation (natural and artificial) and phosphorus cycle in the hardwater lake, Hydrobiologia, 469, 49–57, 2002.

Fletcher, W. J., Sánchez Goñi, M. F., Allen, J. R. M., Cheddadi, R., Coumbourieu-Nebout, N., Huntley, B., Lawson, I. T., Londeix, L., Magri, D., Margari, V., Müller, U. C., Naughton, F., Novenko, E., Roucoux, K. H., and Tzedakis, P. C.: Millennial-scale variability during the last glacial in vegetation records from Europe, Quaternary Sci. Rev., 29, 2839–2864, 2010.

Griffiths, H. I., Kryštufek, B., and Reed, J. M. (Eds.): Balkan Biodiversity: Pattern and Process in the European Hotspot, Kluwer Academic Publishers, Dordrecht, the Netherlands, 357 pp., 2004.

Grimm, E. C.: TILIA and TILIA-graph: Pollen spreadsheet and graphics programs. Programs and Abstracts, 8th International Palynological Congress, Aix-en-Provence, France, 56 pp., 1992.

Grove, A. T. and Rackham, O.: The Nature of Mediterranean Europe – An Ecological History, Yale University Press, London, 384 pp., 2003.

Harrison, S. P. and Digerfeldt, G.: European lakes as palaeohydrological and palaeoclimatic indicators, Quaternary Sci. Rev., 12, 233–248, 1993.

Heinrich, H.: Origin and consequences of cyclic ice rafting in the northeast Atlantic Ocean during the past 130,000 years, Quaternary Res., 29, 142–152, 1988.

Higham, T., Compton, T., Stringer, C., Jacobi, R., Shapiro, B., Trinkaus, E., Chandler, B., Groning, F., Collins, C., Hillson, S., O'Higgins, P., FitzGerald, C., and Fagan, M.: The earliest evidence for anatomically modern humans in northwestern Europe, Nature, 479, 521–524, doi:10.1038/nature10484, 2011.

Hilgen, F. J.: Astronomical calibration of Gauss to Matuyama sapropels in the Mediterranean and implication for the geomagnetic polarity time scale, Earth Planet. Sc. Lett., 104, 226–244, 1991.

Hollis, G. E. and Stevenson, A. C.: The physical basis of the Lake Mikri Prespa systems: geology, climate, hydrology and water quality, Hydrobiologia, 351, 1–19, 1997.

Jankovská, V. and Komárek, J.: Indicative value of *Pediastrum* and other coccal green algae in paleoecology, Folia Geobot., 35, 59–82, 2000.

Jarvis, A., Reuter, H. I., Nelson, A., and Guevara, E.: Hole-filled SRTM for the globe Version 4, available from the CGIAR-CSI SRTM 90 m Database, available at: http://srtm.csi.cgiar.org (last access: 27 November 2011), 2008.

Komárek, J. and Jankovská, V.: Review of the Green Algal Genus *Pediastrum*; Implication for Pollen-analytical Research, Bibliotheca Phycologica, 108, J. Cramer, Berlin, Stuttgart, 127 pp., 2001.

Kouli, K., Brinkhuis, H., and Dale, B.: *Spiniferites cruciformis*: a fresh water dinoflagellate cyst?, Rev. Palaeobot. Palynol., 113, 273–286, 2001.

Koumouzelis, M., Kozlowski, J. K., Escutenaire, C., Sitlivy, V., Sobczyk, K., Valladas, H., Tisnerat-Laborde, N., Wojtal, P., and Ginter, B.: La fin du Paléolithique moyen et le début du Paléolithique supérieur en Grece: la séquence de la Grotte 1 de Klissoura, L'Anthropologie, 105, 469–504, 2001.

Laskar, J., Robutel, P., Joutel, F., Gastineau, M., Correia, A. C. M., and Levrard, B.: A long-term numerical solution for the insolation quantities of the Earth, Astron. Astrophys., 428, 261–285, doi:10.1051/0004-6361:20041335, 2004.

Leng, M. J., Wagner, B., Boehm, A., Panagiotopoulos, K., Vane, C. H., Snelling, A., Haidon, C., Woodley, E., Vogel, H., Zanchetta, G., and Baneschi, I.: Understanding past climatic and hydrological variability in the Mediterranean from Lake Prespa sediment isotope and geochemical record over the Last Glacial cycle, Quaternary Sci. Rev., 66, 123–136, doi:10.1016/j.quascirev.2012.07.015, 2013.

Levin, I. and Kromer, B.: The tropospheric $^{14}CO_2$ level in mid-latitudes of the Northern Hemisphere (1959–2003), Radiocarbon, 46, 1261–1272, 2004.

Lézine, A. M., von Grafenstein, U., Andersen, N., Belmecheri, S., Bordon, A., Caron, B., Cazet, J. P., Erlenkeuser, H., Fouache, E., and Grenier, C.: Lake Ohrid, Albania, provides an exceptional multi-proxy record of environmental changes during the last glacial–interglacial cycle, Palaeogeogr. Palaeocl., 287, 116–127, doi:10.1016/j.palaeo.2010.01.016, 2010.

Lisiecki, L. E. and Raymo, M. E.: A Pliocene-Pleistocene stack of 57 globally distributed benthic $\delta^{18}O$ records, Paleoceanography, 20, PA1003, doi:10.1029/2004PA001071, 2005.

Lowe, J., Barton, N., Blockley, S., Ramsey, C. B., Cullen, V. L., Davies, W., Gamble, C., Grant, K., Hardiman, M., Housley, R., Lane, C. S., Lee, S., Lewis, M., MacLeod, A., Menzies, M., Muller, W., Pollard, M., Price, C., Roberts, A. P., Rohling, E. J., Satow, C., Smith, V. C., Stringer, C. B., Tomlinson, E. L., White, D., Albert, P., Arienzo, I., Barker, G., Boric, D., Carandente, A., Civetta, L., Ferrier, C., Guadelli, J. L., Karkanas, P., Koumouzelis, M., Müller, U. C., Orsi, G., Pross, J., Rosi, M., Shalamanov-Korobar, L., Sirakov, N., and Tzedakis, P. C.: Volcanic ash layers illuminate the resilience of Neanderthals and early modern humans to natural hazards, P. Natl. Acad. Sci. USA, 109, 13532–13537, doi:10.1073/pnas.1204579109, 2012.

Martrat, B., Grimalt, J. O., Shackleton, N. J., de Abreu, L., Hutterli, M. A., and Stocker, T. F.: Four climate cycles of recurring deep and surface water stabilizations on the Iberian margin, Science, 317, 502–507, doi:10.1126/science.1142964, 2007.

Matzinger, A., Jordanoski, M., Veljanoska-Sarafiloska, E., Sturm, M., Müller, B., and Wüest, A.: Is Lake Prespa jeopardizing the ecosystem of ancient Lake Ohrid?, Hydrobiologia, 553, 89–109, doi:10.1007/s10750-005-6427-9, 2006.

Mellars, P.: Neanderthals and the modern human colonization of Europe, Nature, 432, 461–465, doi:10.1038/nature03103, 2004.

Mellars, P.: Why did modern human populations disperse from Africa ca. 60,000 years ago? A new model, P. Natl. Acad. Sci. USA, 103, 9381–9386, 2006.

Mellars, P.: Palaeoanthropology: The earliest modern humans in Europe, Nature, 479, 483–485, 2011.

Meyers, P. A.: Preservation of source identification of sedimentary organic matter during and after deposition, Chem. Geol., 144, 289–302, 1994.

Meyers, P. A. and Ishiwatari, R.: Organic matter accumulation records in lake sediments, edited by: Lerman, A., Imboden, D. M., and Gat, J. R., Springer, Berlin, Heidelberg, 279–328, 1995.

Müller, U. C., Pross, J., Tzedakis, P. C., Gamble, C., Kotthoff, U., Schmiedl, G., Wulf, S., and Christanis, K.: The role of climate in the spread of modern humans into Europe, Quaternary Sci. Rev., 30, 273–279, doi:10.1016/j.quascirev.2010.11.016, 2011.

NGRIP Members: High-resolution record of Northern Hemisphere climate extending into the last interglacial period, Nature, 431, 147–151, 2004.

Okuda, M., Yasuda, Y., and Setoguchi, T.: Middle to late pleistocene vegetation history and climatic changes at Lake Kopais, Southeast Greece, Boreas, 30, 73–82, doi:10.1111/j.1502-3885.2001.tb00990.x, 2001.

Paillard, D., Labeyrie, L., and Yiou, P.: Macintosh program performs time-series analysis, EOS Trans. AGU, 77, 379, 1996.

Panagiotopoulos, K., Aufgebauer, A., Schäbitz, F., and Wagner, B.: Vegetation and climate history of the Lake Prespa region since the Lateglacial, Quatern. Int., 293, 157–169, doi:10.1016/j.quaint.2012.05.048, 2013.

Polunin, O.: Flowers of Greece and the Balkans – A Field Guide, Oxford University Press, Oxford, 692 pp., 1980.

Reimer, P. J., Baillie, M. G. L., Bard, E., Bayliss, A., Beck, J. W., Blackwell, P. G., Bronk Ramsey, C., Buck, C. E., Burr, G. S., Edwards, R. L., Friedrich, M., Grootes, P. M., Guilderson, T. P., Hajdas, I., Heaton, T. J., Hogg, A. G., Hughen, K. A., Kaiser, K. F., Kromer, B., McCormac, F. G., Manning, S. W., Reimer, R. W., Richards, D. A., Southon, J. R., Talamo, S., Turney, C. S. M., van der Plicht, J., and Weyhenmeyer, C. E.: IntCal09 and Marine09 Radiocarbon Age Calibration Curves, 0–50,000 years cal BP, Radiocarbon, 51, 1111–1150, 2009.

Richter, J., Hauck, T., Vogelsang, R., Widlok, T., Le Tensorer, J.-M., and Schmid, P.: "Contextual areas" of early Homo sapiens and their significance for human dispersal from Africa into Eurasia between 200 ka and 70 ka, Quatern. Int., 274, 5–24, doi:10.1016/j.quaint.2012.04.017, 2012.

Rohling, E. J. and Hilgen, F. J.: The eastern Mediterranean climate at times of sapropel formation: a review, Geol. Mijnbouw, 70, 253–264, 1991.

Rossignol-Strick, M.: Mediterranean Quaternary sapropels, an immediate response of the African monsoon to variation of insolation, Palaeogeogr. Palaeocl., 49, 237–263, 1985.

Sánchez Goñi, M. F., Turon, J.-L., Eynaud, F., and Gendreau, S.: European Climatic Response to Millennial-Scale Changes in the Atmosphere-Ocean System during the Last Glacial Period, Quaternary Res., 54, 394–403, doi:10.1006/qres.2000.2176, 2000.

Siddall, M., Rohling, E. J., Almogi-Labin, A., Hemleben, C., Meischner, D., Schmelzer, I., and Smeed, D. A.: Sea-level fluctuations during the last glacial cycle, Nature, 423, 853–858, doi:10.1038/nature01687, 2003.

Stockmarr, J.: Tablets with spores used in absolute pollen analysis, Pollen Spores, 13, 615–621, 1971.

Tourloukis, V. and Karkanas, P.: The Middle Pleistocene archaeological record of Greece and the role of the Aegean in hominin dispersals: new data and interpretations, Quaternary Sci. Rev., 43, 1–15, doi:10.1016/j.quascirev.2012.04.004, 2012.

Trinkhaus, E., Moldovan, O., Milota, S., Bilgar, A., Sarcina, L., Athreya, S., Bailey, S. E., Rodrigo, R., Mircea, G., Higham, T., Bronk Ramseyj, C., and van der Plicht, J.: An early modern human from the Pestera cu Oase, Romania, P. Natl. Acad. Sci., 100, 11231–11236, 2003.

Tzedakis, P. C., Lawson, I. T., Frogley, M. R., Hewitt, G. M., and Preece, R. C.: Buffered tree population changes in a quaternary refugium: evolutionary implications, Science, 297, 2044–2047, doi:10.1126/science.1073083, 2002.

Tzedakis, P .C., Frogley, M. R., Lawson, I. T., Preece, R. C., Cacho, I., and de Abreu, L.: Ecological thresholds and patterns of millennial-scale climate variability: The response of vegetation in Greece during the last glacial period, Geology, 32, 109–112, doi:10.1130/G20118.1, 2004.

Vogel, H., Wagner, B., Zanchetta, G., Sulpizio, R., and Rosén, P.: A paleoclimate record with tephrochronological age control for the last glacial-interglacial cycle from Lake Ohrid, Albania and Macedonia, J. Paleolimnol., 44, 295–310, doi:10.1007/s10933-009-9404-x, 2010.

Waelbroeck, C., Labeyrie, L., Michel, E., Duplessy, J. C., McManus, J. F., Lambeck, K., Balbon, E., and Labracherie, M.: Sea-level and deep water temperature changes derived from benthic foraminifera isotopic records, Quaternary Sci. Rev., 21, 295–305, 2002.

Wagner, B., Vogel, H., Zanchetta, G., and Sulpizio, R.: Environmental change within the Balkan region during the past ca. 50 ka recorded in the sediments from lakes Prespa and Ohrid, Biogeosciences, 7, 3187–3198, doi:10.5194/bg-7-3187-2010, 2010.

Wagner, B., Aufgebauer, A., Vogel, H., Zanchetta, G., Sulpizio, R., and Damaschke, M.: Late Pleistocene and Holocene contourite drift in Lake Prespa (Albania/F.Y.R. of Macedonia/Greece), Quatern. Int., 274, 112–121, doi:10.1016/j.quaint.2012.02.016, 2012.

Wetzel, R. G.: Limnology, Lake and River Ecosystems, 3rd Edn., Academic Press, London, 1006 pp., 2001.

Wijmstra, T. A.: Palynology of the first 30 meters of a 120 m deep section in northern Greece, Acta Bot. Neerl., 18, 511–527, 1969.

Wilke, T., Schultheiß, R., Albrecht, C., Bornmann, N., Trajanovski, S., and Kevrekidis, T.: Native *Dreissena* freshwater mussels in the Balkans: in and out of ancient lakes, Biogeosciences, 7, 3051–3065, doi:10.5194/bg-7-3051-2010, 2010.

Woodward, J. C. and Hughes, P. D.: Glaciation in Greece: A New Record of Cold Stage Environments in the Mediterranean, in: Quaternary Glaciations – Extent and Chronology, edited by: Ehlers, J., Gibbard, P. L., and Hughes, P. D., Elsevier, Amsterdam, 175–198, 2011.

Zilhão, J., Trinkaus, E., Constantin, S., Milota, S., Gherase, M., Sarcina, L., Danciu, A., Rougier, H., Ouilès, J., and Rodrigo, R.: The Peştera cu Oase People, Europe's Earliest Modern Humans, in: Rethinking the Human Revolution, edited by: Mellars, P., Boyle, K., Bar-Yosef, O., and Stringer, C., McDonald Institute for Archaeological Research, Cambridge, 249–262, 2007.